Supplemental Material (not copyedited or formatted) for: Matthew C. Kustra, Tyler J. Carrier. 2022. "On the Spread of Microbes That Manipulate Reproduction in Marine Invertebrates." The American Naturalist 200(2). DOI: https://doi.org/10.1086/720282.

Online Supplement:

On the spread of microbes that manipulate reproduction in marine invertebrates

The American Naturalist

Matthew C. Kustra[1,*] and Tyler J. Carrier [2,3,*]

[1] Department of Ecology and Evolutionary Biology, University of California, Santa Cruz, CA USA

[2] GEOMAR Helmholtz Centre for Ocean Research, Kiel, Germany

[3] Zoological Institute, Kiel University, Kiel, Germany

[*] Corresponding authors: mkustra@ucsc.edu; tcarrier@geomar.de

Supplemental Material (not copyedited or formatted) for: Matthew C. Kustra, Tyler J. Carrier. 2022. "On the Spread of Microbes That Manipulate Reproduction in Marine Invertebrates." The American Naturalist 200(2). DOI: https://doi.org/10.1086/720282.

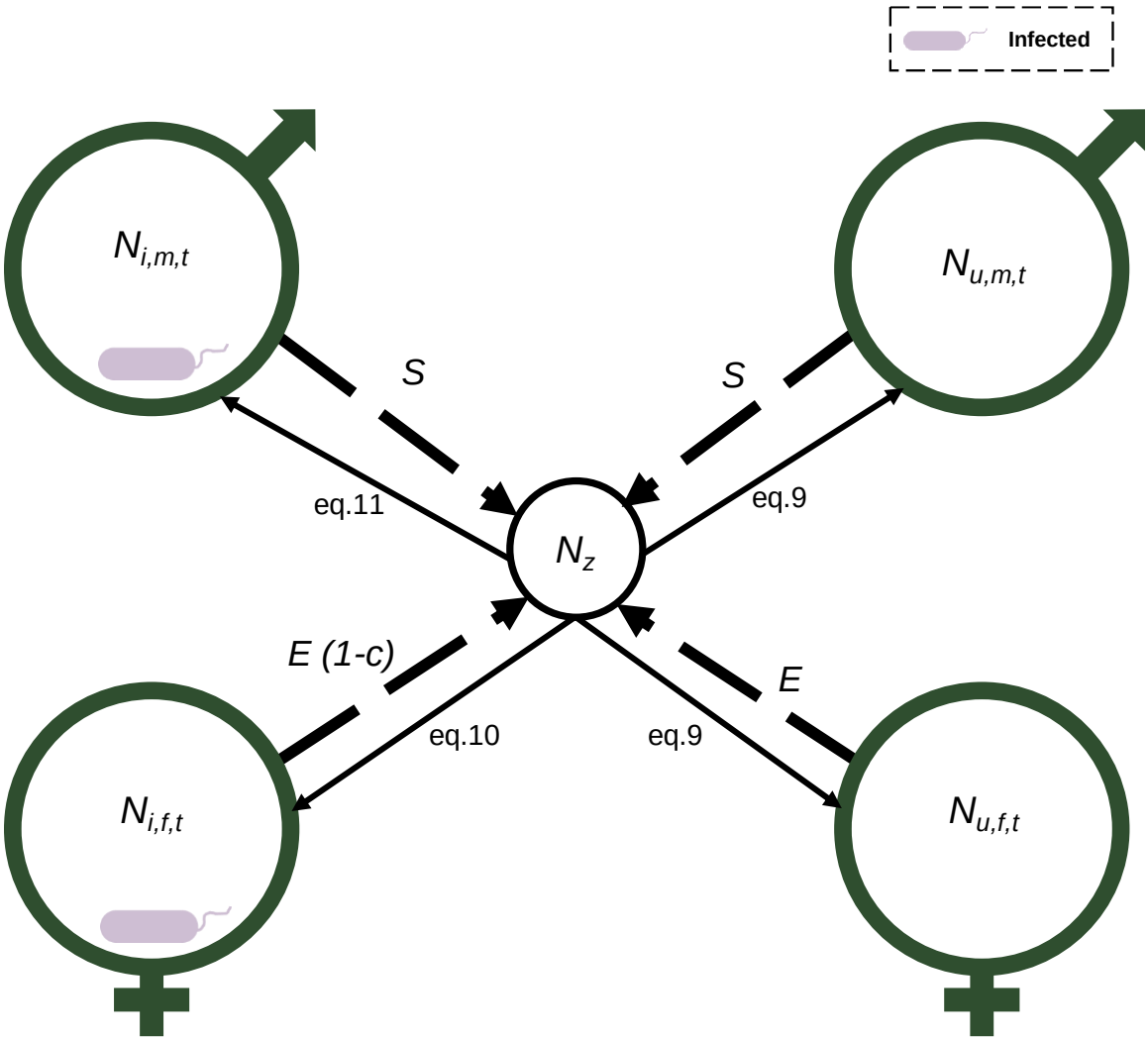

Figure S1. Visualization of the population model without structure that simulates the spread of a reproductive manipulator for free-spawning marine invertebrates. Infected ($N_{i,m,t}$) and uninfected ($N_{u,m,t}$) males both release S amount of sperm, uninfected females ($N_{u,f,t}$) release E amount of eggs, and infected females ($N_{i,f,t}$) release E amount of eggs reduced by the cost of infection (c). The density of zygotes (N_z) is then calculated with Equation 5 and mature into the different groups based on Equations 6-11 in *Spread of reproductive manipulators: no population structure*. Mortality is not explicitly included in this visualization and a full description of model parameters and values are provided in Tables 1 and 2.

Supplemental Material (not copyedited or formatted) for: Matthew C. Kustra, Tyler J. Carrier. 2022. "On the Spread of Microbes That Manipulate Reproduction in Marine Invertebrates." The American Naturalist 200(2). DOI: https://doi.org/10.1086/720282.

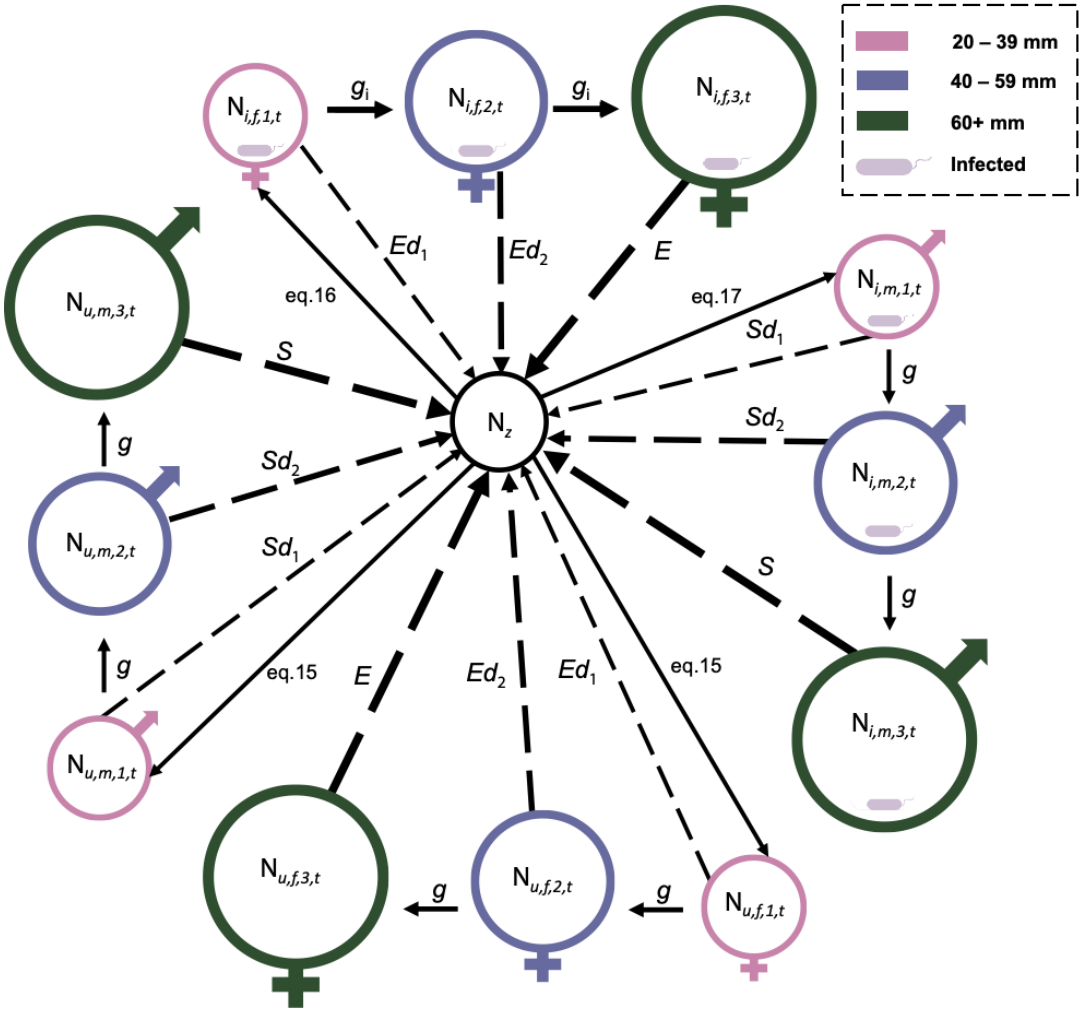

Figure S2. Visualization of the population model with structure that simulates the spread of a microbial reproductive manipulator for the free-spawning sea urchin *Heliocidaris erythrogramma* (see, Equations 6-7 and 12-20). Largest class of females (dark green) produce *E* density of eggs and the largest class of males (dark green) produce *S* amount of sperm. Individuals of both sexes at the middle size class (purple) produce gametes at a reduction factor of (d_2) and the smallest size class (pink) produce gametes at factor of (d_1), such that d_2 is greater than d_1. The density of zygotes (N_z) is then calculated with Equation 5 and mature into the smallest size groups based on the Equations 12-20 in *A case study simulation:* Heliocidaris *with population structure*. After mortality (not shown), a proportion of individuals transition into the next size class. Enhanced growth is incorporated by having the rate of transition to the larger size class (g_i) be greater for infected females than for all other groups (g). All individuals that did not transition to the next size class remain in their size class (not shown). Description of model parameters and values are given in Tables 1, 2, and 3.

Supplemental Material (not copyedited or formatted) for: Matthew C. Kustra, Tyler J. Carrier. 2022. "On the Spread of Microbes That Manipulate Reproduction in Marine Invertebrates." The American Naturalist 200(2). DOI: https://doi.org/10.1086/720282.

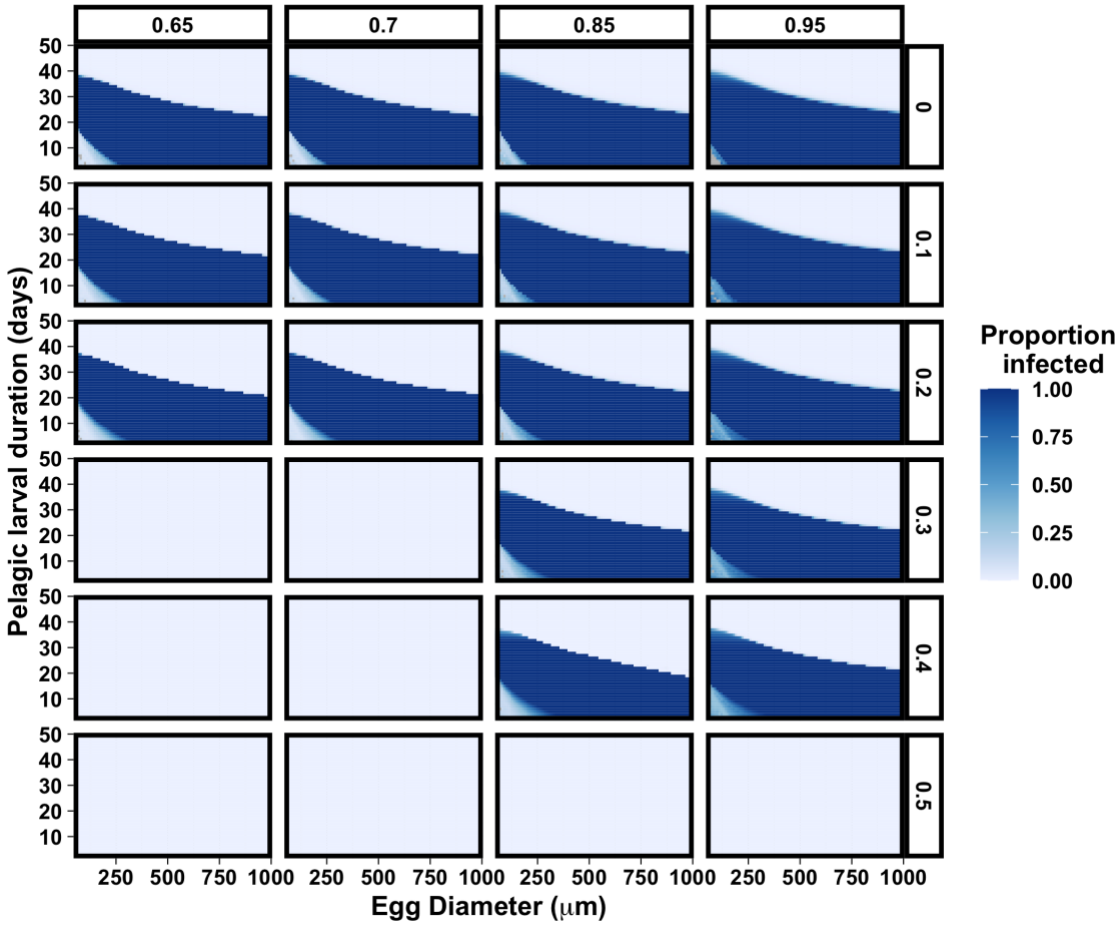

Figure S3. Equilibrium infection rate by a microbe that induces feminization at different combinations of egg diameter (from 40 to 1,000 μm with 10 μm increments) and pelagic larval duration (from 0 to 50 days with 1-day increments) across different combinations of feminization rate (columns) and cost of infection (rows). Numerical simulations to find the equilibrium were performed using Equations 6-11. Light and dark blue represent 0 to 100% infected and grey-shaded boxes indicate parameter combinations that resulted in a "NA" due to too high of a growth rate. For this model, egg density was inversely proportional to egg diameter (Smith & Fretwell 1974). Other parameters of the model were held to be the same as *Heliocidaris erythrogramma* (see, Table 1).

Supplemental Material (not copyedited or formatted) for: Matthew C. Kustra, Tyler J. Carrier. 2022. "On the Spread of Microbes That Manipulate Reproduction in Marine Invertebrates." The American Naturalist 200(2). DOI: https://doi.org/10.1086/720282.

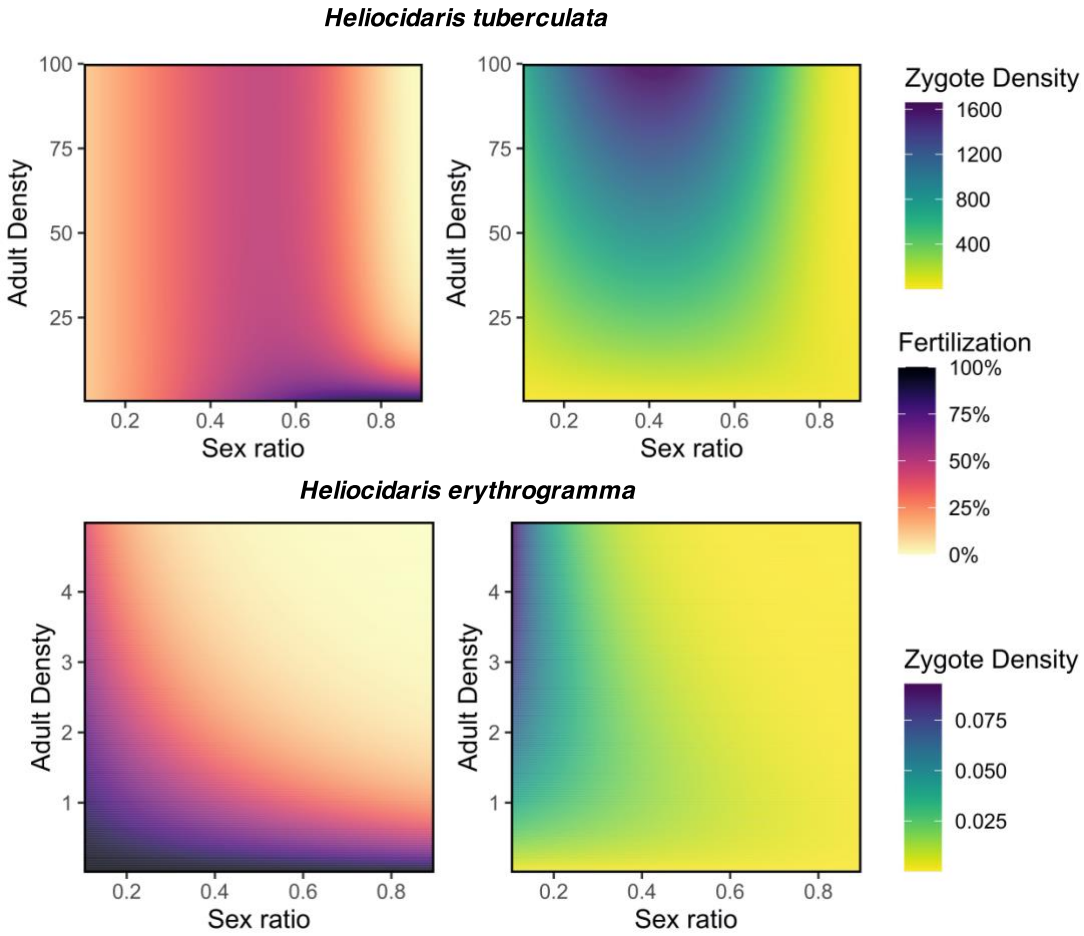

Figure S4. Modeled fertilization dynamics expanding on Figure 1 for two species of free-spawning marine invertebrates with alternative life-history strategies. Fertilization percentage (proportion of eggs fertilized by one sperm; left) and zygote density (zygotes per µL produced in a spawning event; right) for the planktotrophic *Heliocidaris tuberculata* (top) and lecithotrophic *H. erythrogramma* (bottom) at all combinations of adult density (from 0.005 to 100 individuals per m^2 with increments of 0.005) and sex ratio [0.1(female biased) to 0.9 (male biased) with increments of 0.005]. Range of adult density for *H. erythrogramma* is restricted to 5 as densities greater than this generally resulted in zero fertilization percent. Intensity of color indicate either higher fertilization percentage or higher zygote density production. Upper zygote density color scale corresponds to *H. tuberculata* subplot; bottom zygote density color scale corresponds to *H. erythrogramma* subplot. Equations 4 and 5 used to generate this figure were adopted from the Styan (1998) polyspermy model and uses species-specific parameters from the literature (Table 1).

Supplemental Material (not copyedited or formatted) for: Matthew C. Kustra, Tyler J. Carrier. 2022. "On the Spread of Microbes That Manipulate Reproduction in Marine Invertebrates." The American Naturalist 200(2). DOI: https://doi.org/10.1086/720282.

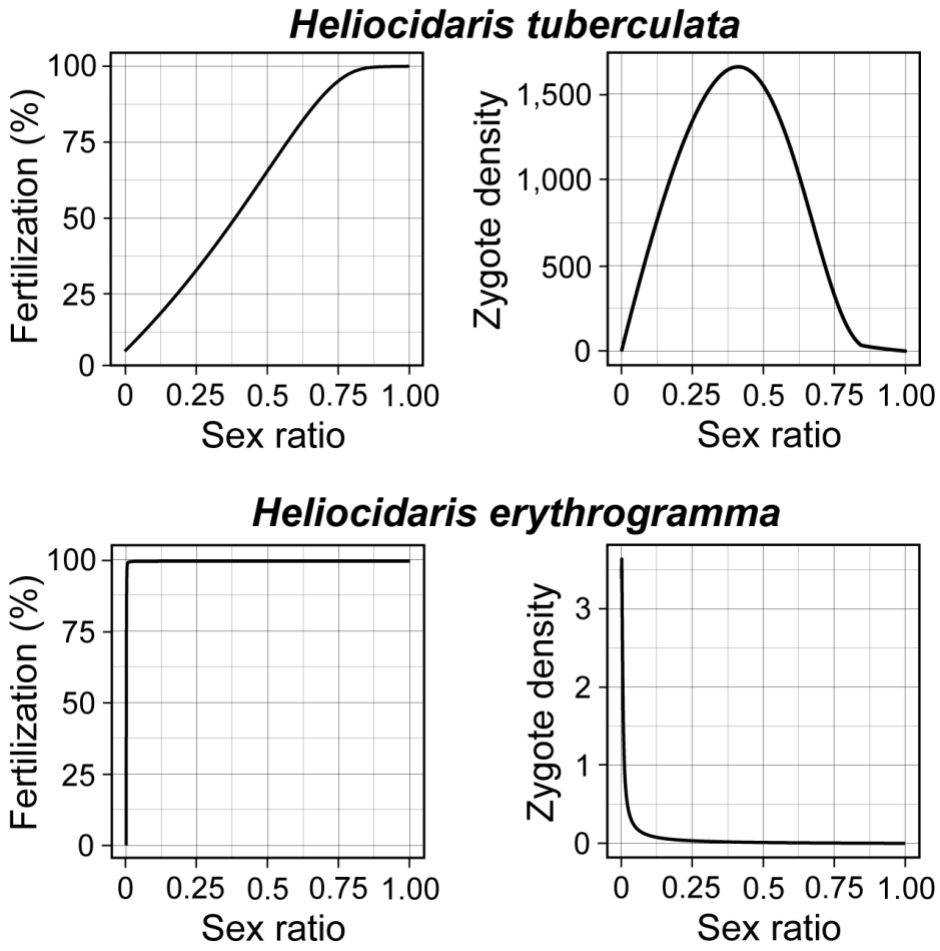

Figure S5. Maximum fertilization success and zygote density (zygotes per μL) across sex ratios for both *Heliocidaris tuberculata* (top) and *H. erythrogramma* (bottom). Based on Figure 1, this depicts the highest fertilization percent and zygote density possible at each sex ratio [from 0 (all females) to 1 (all males) with increments of 0.001] within an adult density range from 0 to 100 individuals per m^2 with increments of 0.0001. Note that the maximum fertilization percent and the maximum zygote density were often not at the same adult density (Figure S4). Equations 4 and 5 used to calculate fertilization percent and zygote density were adopted from the Styan (1998) polyspermy model and used species-specific parameters from the literature (Table 1). The reproductive parameters for Figure 1 can be altered to generate additional species-specific curves in the supplemental web application. Please note that the maximum fertilization rate in all female (0) and all male (1) are "NA" and not shown.

Supplemental Material (not copyedited or formatted) for: Matthew C. Kustra, Tyler J. Carrier. 2022. "On the Spread of Microbes That Manipulate Reproduction in Marine Invertebrates." The American Naturalist 200(2). DOI: https://doi.org/10.1086/720282.

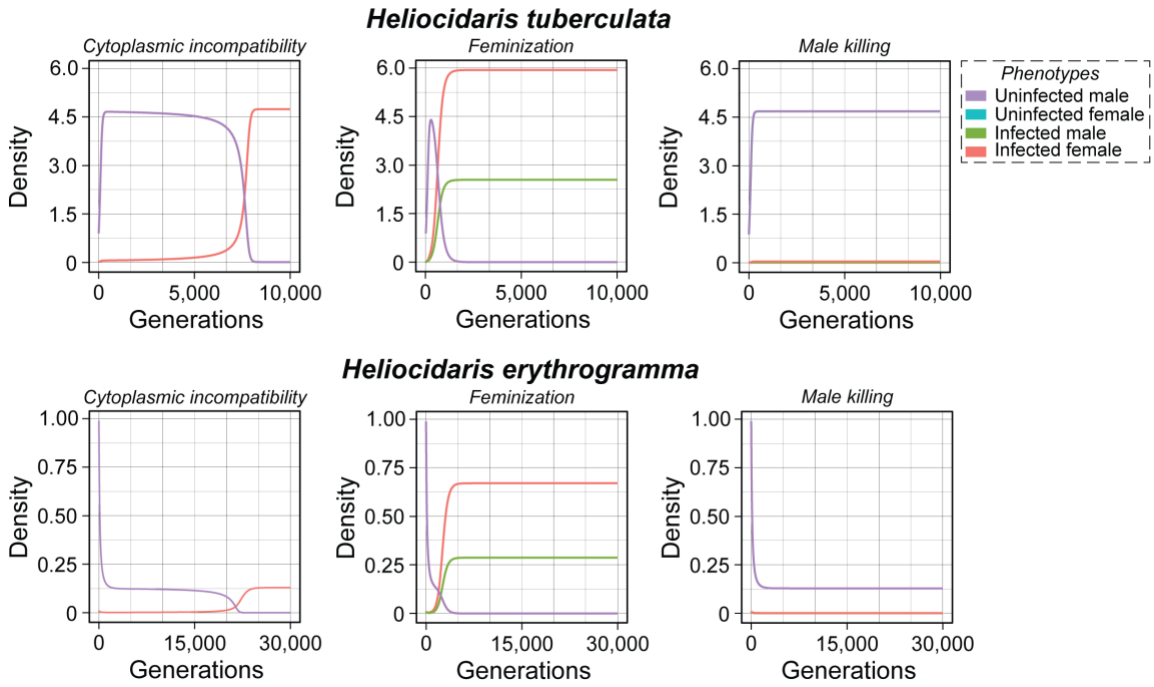

Figure S6. Population structure during the spread of a microbial reproductive manipulator for two species of free-spawning marine invertebrates with alternative life-history strategies. Complementary to Figure 2, these numerical simulations show the density (individuals per m^2) of either uninfected male (purple), uninfected females (blue), infected male (green), or infected females (red) for the planktotrophic *Heliocidaris tuberculata* (top) and lecithotrophic *H. erythrogramma* (bottom) when a microbe that induces cytoplasmic incompatibility (left), feminization (center), and male killing (right) spreads within the population. The lines for uninfected male (purple) and females (blue) overlap for all mechanisms, and the lines for infected males (green) and females (red) overlap under cytoplasmic incompatibility. These simulations use a population model without stage structure (see, Equations 6-11) and start with a naïve population (1% infected). Parameter values used are provided in Tables 1 and 2, and additional simulations can be run using the supplemental web application.

Supplemental Material (not copyedited or formatted) for: Matthew C. Kustra, Tyler J. Carrier. 2022. "On the Spread of Microbes That Manipulate Reproduction in Marine Invertebrates." The American Naturalist 200(2). DOI: https://doi.org/10.1086/720282.

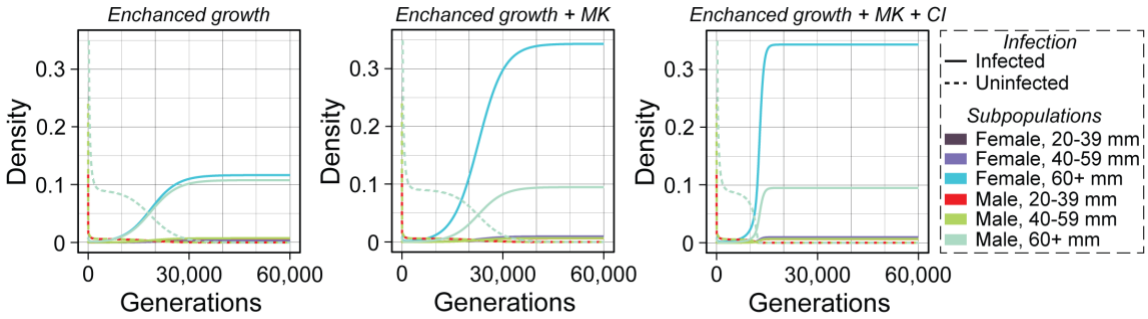

Figure S7. Population structure during the spread of a microbial reproductive manipulator for *Heliocidaris erythrogramma*. Based on Figure 3, these numerical simulations show adult density (individuals per m^2) for both sexes and infection status (*i.e.*, line types) of small (20-39 mm), medium (40-59 mm), and large (60+ mm) individuals when a microbe that enhances growth (left), enhances growth and incudes male killing (center), and enhances growth, incudes male killing, and causes cytoplasmic incompatibility (right) spreads within a population. These simulations use a stage-based population model (see, Equations 6-7 and 12-20) and start with a naïve population (1% infected). Parameter values used are provided in Tables 1, 2, and 3, and additional simulations can be generated using the supplemental web application.

Supplemental Material (not copyedited or formatted) for: Matthew C. Kustra, Tyler J. Carrier. 2022. "On the Spread of Microbes That Manipulate Reproduction in Marine Invertebrates." The American Naturalist 200(2). DOI: https://doi.org/10.1086/720282.

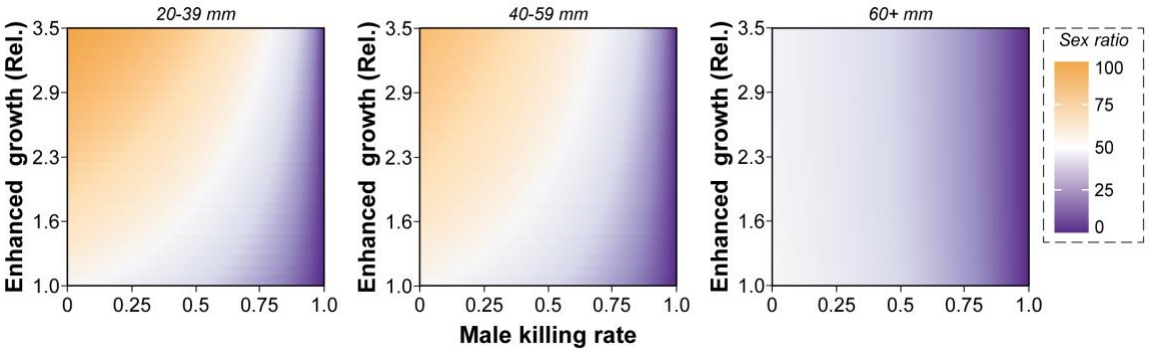

Figure S8. Equilibrium sex ratio (percentage of males) of the three size classes after infection by a male killing microbe across different combinations of relative enhanced growth rate (from 1.1 to 3.5 with 0.1 increments) and male killing rate (from 0 to 0.99 with 0.01 increments). Numerical simulations of the stage-based model to reach the equilibrium were performed using Equations 6-7 and 12-20. Other parameter values used are the same as *Heliocidaris erythrogramma* and provided in Tables 1, 2, and 3.

Supplemental Material (not copyedited or formatted) for: Matthew C. Kustra, Tyler J. Carrier. 2022. "On the Spread of Microbes That Manipulate Reproduction in Marine Invertebrates." The American Naturalist 200(2). DOI: https://doi.org/10.1086/720282.

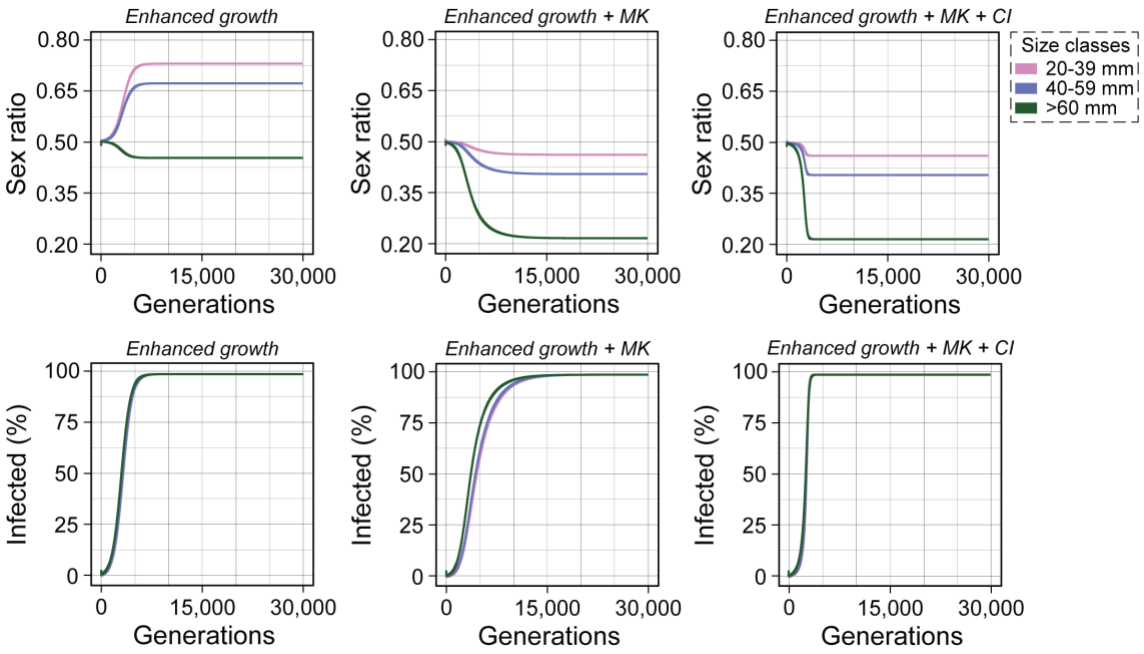

Figure S9: Sex ratio and population structure during the spread of a microbial reproductive manipulator for *Heliocidaris tuberculata*. Numerical simulations of host sex ratio (with male- and female-bias being >0.5 and <0.5, respectively; top) and proportion infected over time (bottom) when a microbe that enhances growth (left), enhances growth and incudes male killing (center), and enhances growth, incudes male killing, and causes cytoplasmic incompatibility (right) spreads within a population. These simulations use a stage-based population model and start with a naïve population (1% infected) where all individuals are in the smallest size class (see, Equations 6-7 and 12-20). Parameter values used are provided in Tables 1, 2, and 3, and additional simulations can be generated using the supplemental web application.

Supplemental Material (not copyedited or formatted) for: Matthew C. Kustra, Tyler J. Carrier. 2022. "On the Spread of Microbes That Manipulate Reproduction in Marine Invertebrates." The American Naturalist 200(2). DOI: https://doi.org/10.1086/720282.

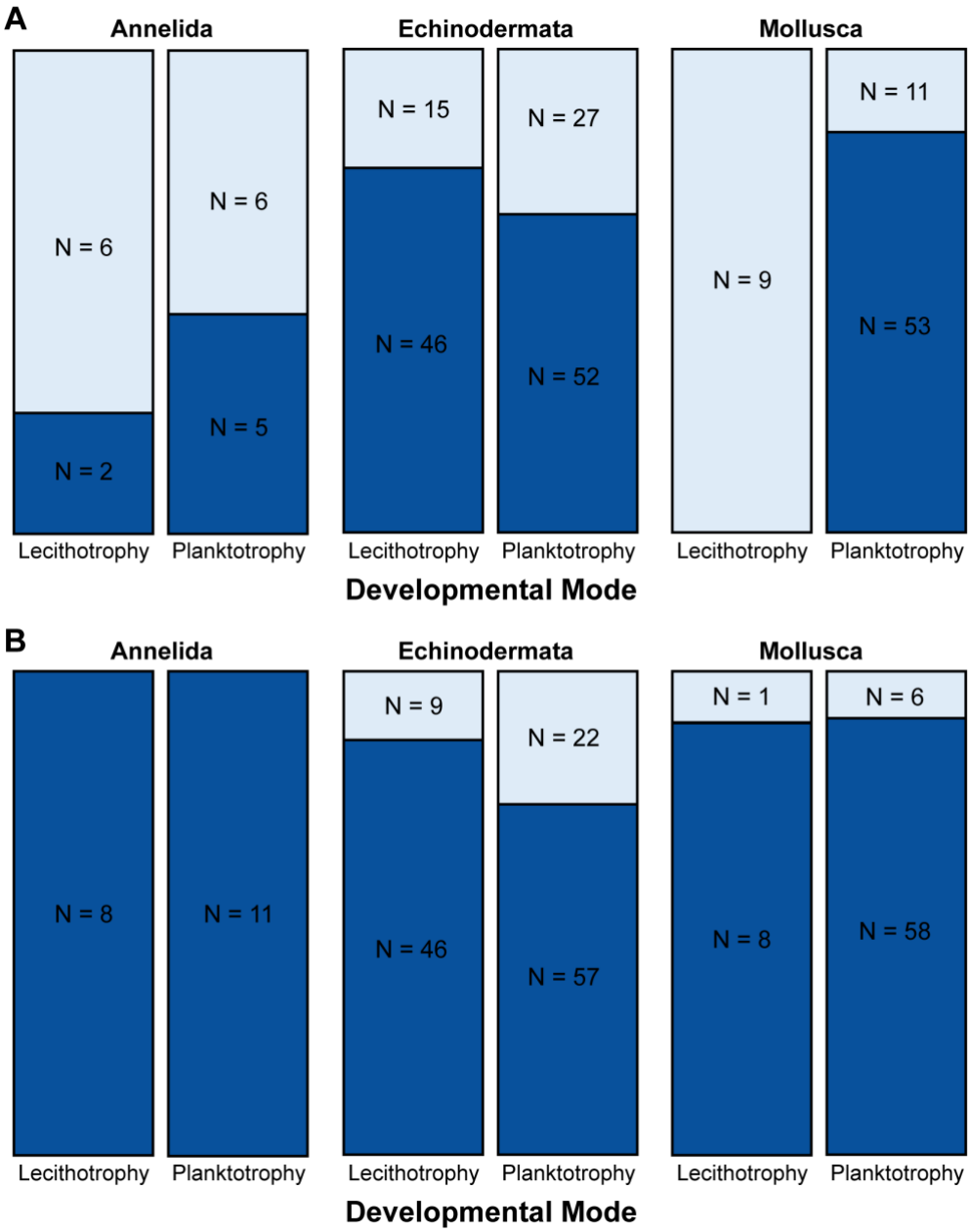

Figure S10. Proportion of marine invertebrate species predicted to be infectable by a microbe that elicits (A) feminization or (B) males killing plus enhanced growth, as based on the numerical simulations in Figure 4 and the datasets in Álvarez-Noriega et al. (2020) and Marshall et al. (2012). These species were divided by Phylum (Annelida, Echinodermata, and Mollusca) and subdivided by developmental mode (planktotrophy and lecithotrophy). Proportion of species predicted to be infectible are shown in dark blue while those predicted to be uninfectable are shown in light blue. Species that did not have available data for both traits were not shown and both Chordata and Cnidaria phyla were excluded due a limited number of species with available data. The location of marine invertebrate species based on these two life-history parameters can be explored in the supplemental web application.

Supplemental Material (not copyedited or formatted) for: Matthew C. Kustra, Tyler J. Carrier. 2022. "On the Spread of Microbes That Manipulate Reproduction in Marine Invertebrates." The American Naturalist 200(2). DOI: https://doi.org/10.1086/720282.

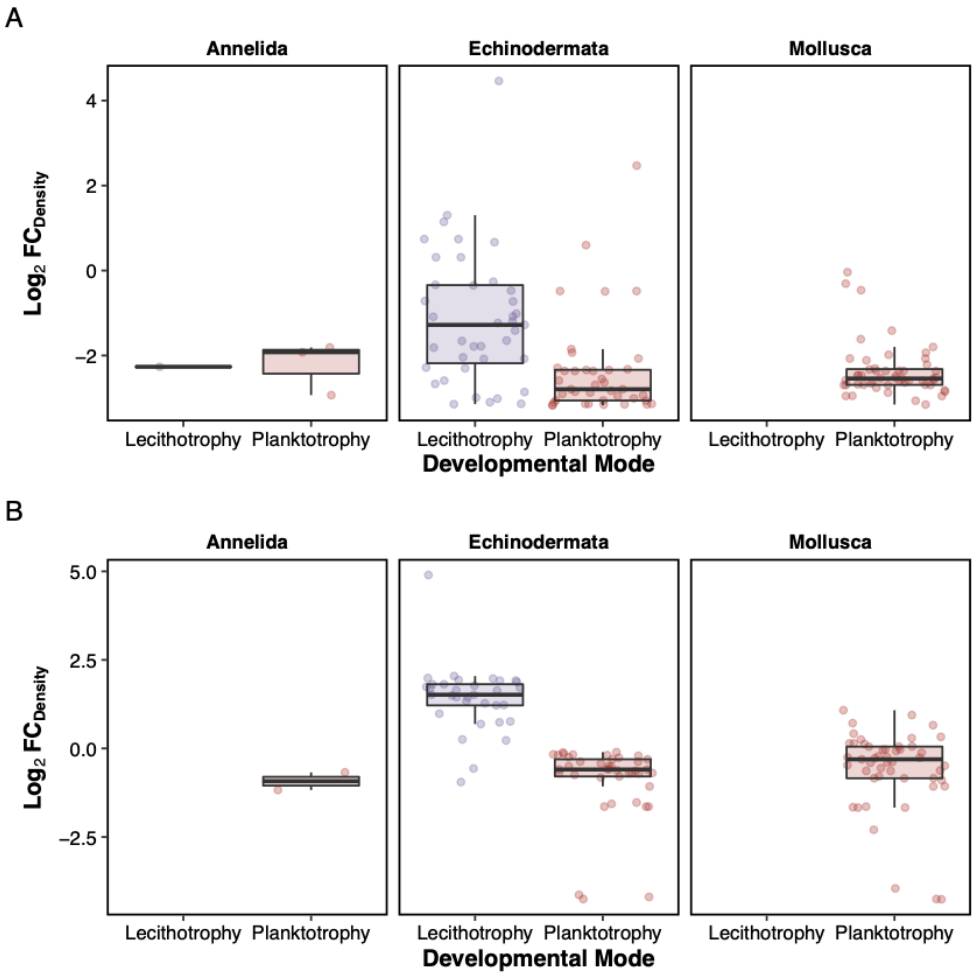

Figure S11. Predicted $\log_2$ fold change in density (individuals per m^2) of marine invertebrates that are predicted to be infectable by a microbe that elicits (A) feminization or (B) male killing plus enhanced growth, as based on the numerical simulations in Figure 4 and the datasets in Álvarez-Noreiga et al. (2020) and Marshall et al. (2012). These species were divided by Phylum (Annelida, Echinodermata, and Mollusca) and subdivided by developmental mode (planktotrophy and lecithotrophy. Species that were not predicted to be infected or were extreme outliers (absolute $\log_2$ fold change > 25) are not shown.